Change in spectrogram of acoustic emission under the uniaxial compression loading of polymer cement mortar due to the porosity

Takanori Ito
Graduate School of General Science – Iwate University, Morioka, Iwate, Japan
Kiyohito Yamamoto & Motohei Kanayama
Faculty of Agriculture – Iwate University, Morioka, Iwate, Japan
Yuki Sato, Takeshi Suzuki & Noriaki Takahashi
Daiichi Kensetsu Co,.LDH, Chuo-ku, Niigata, Japan

ABSTRACT
Many landslides happen every year in Japan. The landslide is caused by torrential downpour or degradation of the slope. The fatal accident by a landslide due to torrential downpour can be avoided if the attention is focused on during and after rain. However, the collapse due to the degradation of the rocks is very difficult to predict. In this study, the acoustic emission (AE) behavior of polymer cement mortar (PCM) under the uniaxial compression loading due to the difference in porosity was investigated.

Degraded specimens were prepared by mixing the expansive additive with PCM to simulate a porous rock, and sound specimens are the PCM without the additive. Measurements of AE were performed using an AE transducer and the signal was recorded by a PC-based digital oscilloscope. The AE signal and strain, load were measured in a uniaxial compression test. The spectrogram was created from the AE signal using a short-time Fourier transform every second.

The AE characteristics of the degraded specimen were examined, comparing spectrograms on the entire loading process from unloading to failure. The following results were obtained:

(1) For the degraded specimens, many AE signals with large amplitude occurred from initial loading to failure. On the other hand, for the sound specimens, there was a little AE signal until the maximum volumetric strain, the number and amplitude of that drastically increased close to failure.

(2) The spectrogram of the degraded specimens had a large amplitude in a relatively wide frequency band from the initial loading. In the spectrogram of the sound specimens, the frequency band with large amplitude gradually increased from the maximum volumetric strain.

(3) The degraded specimens tended to have a larger axial strain of maximum stress and larger maximum volumetric strain than the sound one. In addition, for the degraded specimens, the time between maximum volumetric strain and failure became longer.

RÉSUMÉ
De nombreux glissements de terrain se produisent chaque année au Japon. Le glissement de terrain est causé par une averse torrentielle ou une dégradation de la pente. Les accidents de glissement de terrain causés par des pluies torrentielles peuvent être évités si l'on fait attention pendant et après la pluie. Cependant, l'effondrement dû à la dégradation des roches est très difficile à prévoir. Dans cette étude, le comportement d'émission acoustique (AE) du mortier de ciment polymère (PCM) sous la charge de compression uniaxiale due à la différence de porosité a été étudié.
Des spécimens dégradés ont été préparés en mélangeant un additif expansif avec du PCM pour simuler une roche poreuse, et les spécimens sains sont le PCM sans l'additif. Les mesures de l'AE ont été effectuées à l'aide d'un transducteur AE et le signal a été enregistré par un oscilloscope numérique basé sur PC. Le signal AE et la déformation, la charge ont été mesurés dans un test de compression uniaxiale. Le spectrogramme a été créé à partir du signal AE en utilisant une transformée de Fourier à court terme toutes les secondes.
Les caractéristiques AE des spécimens dégradés ont été examinées, en comparant les spectrogrammes sur l'ensemble du processus de chargement, du déchargement à la rupture. Les résultats suivants ont été obtenus:
(1) Pour l'échantillon dégradé, de nombreux signaux AE de grande amplitude se sont produits du chargement initial à la défaillance. En revanche, pour l'échantillon sonore, il y avait un petit signal AE jusqu'à la déformation volumétrique maximale, dont le nombre et l'amplitude ont considérablement augmenté près de la rupture.
(2) Le spectrogramme de l'échantillon dégradé avait une grande amplitude dans une bande de fréquence relativement large à partir du chargement initial. Dans celui de l'échantillon sonore, la bande de fréquence de grande amplitude augmente progressivement à partir de la déformation volumétrique maximale.
(3) L'éprouvette dégradée avait tendance à avoir une plus grande déformation axiale de contrainte maximale et une plus grande déformation volumétrique maximale que celle en bon état. De plus, pour l'éprouvette dégradée, le temps entre la déformation volumétrique maximale et la rupture est devenu plus long.

1 INTORODUCTION

Many landslides happen every year in Japan. The landslide is caused by torrential downpour or degradation of the slope. The fatal accident by a landslide due to torrential downpour can be avoided if the attention is focused on during and after rain. However, the collapse due to the degradation of the rocks is very difficult to predict.

The acoustic emission (AE) technique is used as a health monitoring method for concrete structures. *AE refers to the generation of transient elastic waves produced by a sudden redistribution of stress in a material. When a structure is subjected to an external stimulus (change in pressure, load, or temperature), localized sources trigger the release of energy, in the form of stress waves, which propagate to the surface and are recorded by sensors* (Motahari-Nezhad et al. 2020).

In this study, the purpose is to investigate the failure process of brittle materials such as concrete, mortar, and rock. Firstly, specimens of polymer cement mortar (PCM) mixed with different amounts of the expansive additive were prepared, and the deformation behaviors of those specimens were observed during curing. Secondly, the elastic wave velocities of specimens were measured, and the mechanical behaviors were investigated by performing a uniaxial compression test. The Poisson's ratio and Young's modulus were calculated from the load and strain measured by the compression tests. The AE signals were continuously recorded during the compression test from unloading to failure, and the signals were processed using a short-time Fourier transform every second to create a spectrogram. After the test, the density and porosity of the specimens were measured with a water absorption test. Finally, the mechanical and AE behaviors of PCM specimens with different porosities were investigated by comparing these results to examine the behavior of failure for brittle materials.

2 METHODS

2.1 Materials and Specimens

Cylindrical specimens with a diameter of 5 cm and a height of 10 cm were prepared. The specimens were made of PCM and water, and those porosities were changed by the expansive additive. PCM consists of cement, fine aggregate, and polymer. *Zhang et al. (2018) confirmed that Expansive additive cause the formation of expansive substances, calcium hydroxide and ettringite contribute to the occurrence of delayed expansion and the autogenous shrinkage of specimens was effectively decreased by increasing the proportion of the expansive additive*. The Expansive additive was added to PCM and mixed with water by hand kneading. After that, the material was packed in 6 layers in the mold of a cylindrical tin can, and each layer was compacted with a table vibrator. The end face of the mold was smoothed with a straight edge and held down with a metal plate and left until the next day's demolding. Therefore, the end face on one side of the specimen is not completely smooth.

Specimens with different porosities were prepared by the expansive additive, and 3 types of formulations shown in Table 1 were set to examine the effect on uniaxial compression behavior, and 2 specimens of each formulation were prepared. “A” of mix in Table 1 shows not added with expansive additive, “B” shows added in an appropriate amount, and “C” shows excessively added.

Table 1. Mix proportion of polymer cement mortar (PCM)

Mix	Mass per unit volume (kg/m^3)			Expansive additive (kg)
	Water	PCM dry powder		
		Cement	Fine aggregate and polymer	
A	220	525	1575	0
B	220	525	1575	20
C	220	525	1575	40

2.2 Deformation measurement of the specimen exposed to air during curing

The strain of the specimens was measured to investigate the expansion and shrinkage behavior during curing. The day after the mortar was molded, it was removed, and strain gauges (Kyowa electronic Instruments, KFGS-30-120) were installed in the center of the specimen surface in the height direction. The length of the strain gauge is 30mm, and the adhesive (Kyowa electronic Instruments, CC-35) was used for the installation. Strains of specimens from 1 to 66 days of age were recorded every 2 hours with a data logger (Keyence, NR-600, and NR-ST04). During the strain recording, the specimens were left in a dry room during the winter, which is an especially difficult environmental condition for air-curing.

2.3 Uniaxial compression test

A uniaxial compression test was carried out to investigate the mechanical behavior of the PCM specimen. The strain of the specimen was measured via the strain gauge and the load was measured via a load cell (A&D, CM-10). The data of load and strain were recorded with the data logger at a sampling interval of 10 ms. The strain gauges were installed with the adhesive in the circumferential direction and the axial (height) direction at the center of the specimen, as shown in Figure 1. The age of the specimens was 93 days at the time of the test. The specimens were loaded with rubber capping on the end face of the specimen on one side since the side was not smooth.

Young’s modulus (E_{33}), Poisson's ratio (ν_{33}), compression strength ($f'c$), axial strain at maximum stress (ε_{amax}), and maximum volumetric strain (ε_{vmax}) were obtained from the test results. The axial and circumferential strain is the average of the strain gauge measurements installed at each of the two locations. Poisson's ratio was calculated from the strain data recorded at 1/3 of the maximum stress. Young’s modulus was calculated from the strain and load data at 1/3 of the maximum stress and the axial strain close

to 50x10^{-6}. The volumetric strain was calculated by adding the axial strain plus twice the circumferential strain.

Before the uniaxial compression test, the elastic wave velocity (*Vp*) was measured using an AE measuring apparatus. The AE signals were recorded with the digital oscilloscope (NI, PXIe-5105) via two AE sensors (Fuji Ceramics, AE503S) placed with silicon grease (Shin-Etsu Chemical, G30M) at both ends of the specimen as voltage waveforms. A mechanical pencil lead was placed in contact with one end face, the lead was folded, and the elastic wave was recorded as an AE signal. The arrival time of elastic waves propagating inside the specimen was read from the waveform displayed on the PC monitor. *Vp* was obtained from the difference in arrival times and the distance between the sensors. The water content (*w*) was measured from the fractured specimen pieces after the test. Furthermore, the wet density (*ρw*), dry density (*ρd*), effective porosity (*n*), and water absorption rate (*Q*) were measured from the mass and weight in water of the specimen pieces saturated by submerging the piece in water for 7 days or more and from the mass of the dried specimen pieces.

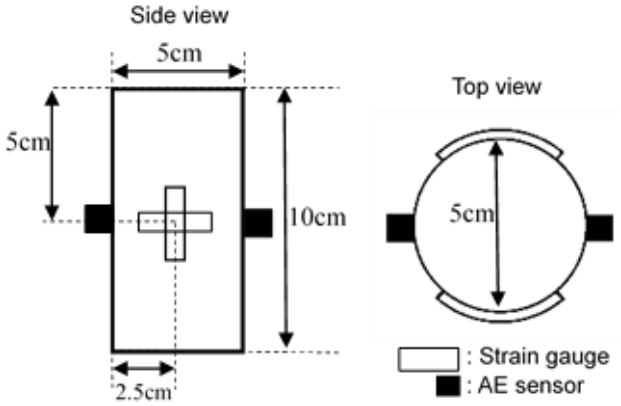

Figure 1. Installation position of strain gauge and AE sensor

2.4 AE measurement

AE signals were recorded during the uniaxial compression test to investigate the AE behavior under the loading from unloading to failure. The AE sensors were installed with silicon grease on the side surface of the specimen as shown in Figure 1. The AE signals were continuously recorded with the digital oscilloscope as voltage data in the PC storage device. The sampling frequency is 10 MHz.

The time-series voltage data was processed with a short-time Fourier transform every 0.839 seconds to create the spectrogram. The Fourier transform was performed by a library program (Massachusetts Institute of Technology, FFTW3). The amplitude (a_i) was calculated by squaring the imaginary part and the real part, dividing the square root of their sum by the number of samples, and doubling it. Decibel-volt unit (dBV) was converted from the voltage unit (dBV) by the following “Eq.1”.

$$Ai = 20\log_{10} a_i \quad [1]$$

The target frequency range is 10 kHz to 500 kHz in this study. This is because the high-pass filter of the preamplifier (NF, 9913) is 10 kHz and there is a special amplitude peak around 591 kHz that may be environmental noise. Since the amplitude data is enormous, here the averages were obtained for each 1 kHz interval and arranged in time series to create a spectrogram. Since the AE data and the load and strain data are recorded on different PCs, time synchronization is necessary. Here, the voltage data of the square wave (frequency 5Hz, voltage ± 2V) of the function generator was recorded on both PCs at the beginning and end of the test, and this was used as the synchronization signal.

3 RESULTS

3.1 Expansion and shrinkage behavior of the specimen exposed to air during curing

Figure 2 shows the strain measurement results of the specimens exposed to air during curing. The tendency of expansion and shrinkage behavior of the specimens for each mix proportion will be discussed.

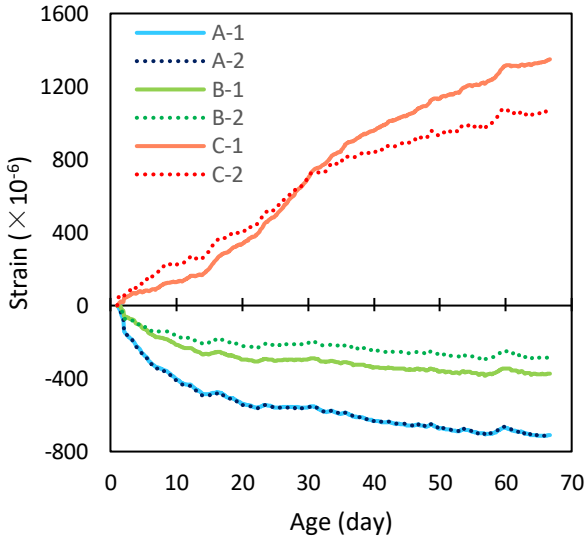

Figure 2. Results of strain measurement of polymer cement mortar specimens exposed to indoor air

Expansion is a positive value. In the legend of the figures, the letter before the hyphen "-" indicates the type of mix proportion, and the number after the hyphen "-" indicates the identification number of the specimen.

A specimens, to which no expansive additive was added, exhibited similar expansion and shrinkage behavior in the two specimens. The maximum amount of shrinkage was observed in comparison with the specimens of the other mix proportion. Strain behavior was significantly different between the B specimens with moderate and C specimens with excessive additive. Shrinkage was observed in the B specimens and expansion was observed in the C specimens.

B specimens showed shrinkage behavior from the beginning of the measurement as in the A specimens, but the amount of shrinkage was small. On the other hand, C

Table 2. Test results

Specimen	f'_c (MPa)	ε_{amax} ($\times10^{-6}$)	ε_{vmax} ($\times10^{-6}$)	E_{33} (GPa)	v_{33}	V_p (m/s)	w (%)	ρ_w (g/cm^3)	ρ_s (g/cm^3)	Q (%)	n (%)
A-1	41.3	2617	972	22.1	0.19	4263	2.42	2.27	2.11	7.57	16.0
A-2	44.0	3032	1004	23.0	0.19	4409	2.42	2.26	2.10	7.71	16.2
B-1	46.2	2952	985	22.1	0.19	4609	2.49	2.24	2.08	7.77	16.2
B-2	44.1	3221	933	21.6	0.19	4395	2.46	2.22	2.06	7.95	16.4
C-1	36.1	3691	1172	11.8	0.15	3045	2.56	2.18	2.01	8.97	18.0
C-2	38.4	3858	1241	11.8	0.14	3099	2.63	2.19	2.02	8.63	17.4

specimens showed expansion behavior.
For B specimens, the amount of strain contraction decreases with increasing age, while for C specimens, the amount of strain expansion and age continue to increase at a linearly constant rate.

Therefore, the C specimens are degraded specimens with many pores inside, while the A specimens simulate a sound specimen with a large amount of shrinkage.

3.2 Mechanical parameters

Table 2 shows compressive strength (f'_c), axial strain at maximum stress (ε_{amax}), maximum volumetric strain (ε_{vmax}), compressive secant Young's modulus (E_{33}), secant Poisson's ratio (v_{33}), elastic wave velocity (Vp), water content ratio (w), wet density (ρ_w), dry density (ρ_s), water absorption (Q), and effective porosity (n). The mechanical properties will be discussed by comparing the mechanical parameters between the A specimens and the other specimens.

In C specimens, the compressive strength (f'_c), compressive secant Young's modulus (E_{33}), secant Poisson's ratio (v_{33}), elastic wave velocity (Vp), wet density (ρ_w), and dry density (ρ_s) decreased. Axial strain at maximum stress (ε_{amax}), maximum volumetric strain (ε_{vmax}), water absorption (Q), and effective porosity (n) increased. These results suggest that the excessive voids inside the specimen caused by the expansive additive are responsible for the decrease in strength and stiffness and the increase in compressibility. On the other hand, the B specimens showed a slight increase in compressive strength (f'_c) and water absorption (Q) and a decrease in density, however, no significant differences in mechanical parameters such as compressive strength were observed.

3.3 Stress, volumetric strain and AE behavior under the uniaxial compression loading

Figure 3 shows the stress and volumetric strain behavior of the A-1 specimen, and Figure 4 shows a spectrogram of the AE behavior of the A-1 specimen. Two AE sensors were used in the measurement of AE behavior, however, only the results of one sensor are shown because no significant differences were observed in the spectrograms. The horizontal axis of the spectrogram is the time from the start of the measurement. The amplitude indicated by the color is the value calculated by a short-time Fourier transform and averaged every 1 kHz, separated by 0.839 seconds. Similarly, stress, volumetric strain, and AE behavior of the A-2 specimen are shown in Figures 5 and 6, the B-1 specimen in Figures 7 and 8, the B-2 specimen in Figures 9 and 10, and the C-1 specimen in Figures 11 and 12, and the C-2 specimen in Figures 13 and 14.

For the A-1 specimen in Figures 3 and 4, the AE signal was slight up to 241 seconds, when the maximum volumetric strain was measured. However, the number and amplitude of AE signals increased significantly closer to failure. For the A-2 specimen in Figures 5 and 6, AE signals were observed from the beginning of the loading phase. Insufficient compaction at the time of specimen fabrication would cause small-scale failure at an early stage due to the non-uniformity of the density inside the specimen. The maximum volumetric strain was observed at approximately 100 seconds, and a large amplitude region centered at 100 kHz was observed, with the maximum stress at approximately 120 seconds. The distribution at the time of fracture was also widely extended.

The stress and volumetric strain behavior of the B-1 and B-2 specimens in Figures. 7 and 9 showed similar behavior to that of the A specimens. This is because the results of the mechanical parameters in Section 3.2 measured similar values for the A and B specimens, which may explain the similar behavior of each specimen. On the other hand, the B-2 specimen shown in Figure 10 generates slightly more AE signals than the A and B-1 specimens. This is because the B-2 specimen has larger water absorption (Q) and effective porosity (n) than the A and B-1 specimens, and there are many voids in the interior of the B-2 specimen, which may have caused cracks in the interior of the specimen due to loading and generated more AE signals.

Figures 12 and 14 show that the AE behavior of the C specimen with excess expansion material produced many large-amplitude AE signals over a relatively wide frequency range from the early loading stage to failure. In addition, Figures 11 and 13 show that the C specimens measured maximum volumetric strain at an earlier stage than the A and B specimens, and the time from maximum volumetric strain to failure was longer relative to the length of test time. This suggests that more AE signals are generated when there are more voids inside the specimen, and the less rigid the specimen is, the more the fracture progresses inside the specimen and the amplitude becomes larger.

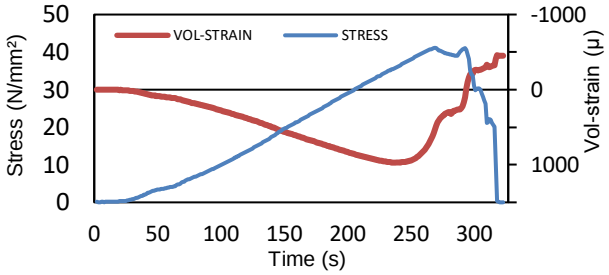

Figure 3. Stress and volumetric strain behavior under uniaxial compression loading (A-1 specimen)

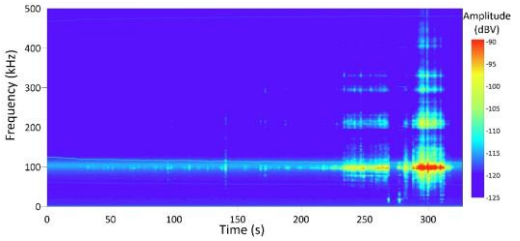

Figure 4. AE behavior under uniaxial compression loading (A-1 specimen)

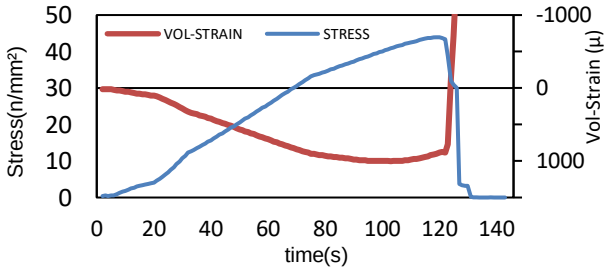

Figure 5. Stress and volumetric strain behavior under uniaxial compression loading (A-2 specimen)

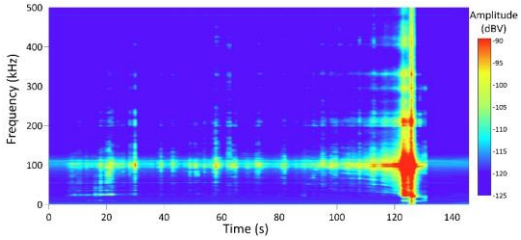

Figure 6. AE behavior under uniaxial compression loading (A-2 specimen)

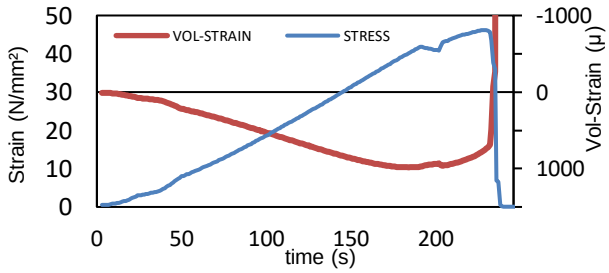

Figure 7. Stress and volumetric strain behavior under uniaxial compression loading (B-1 specimen)

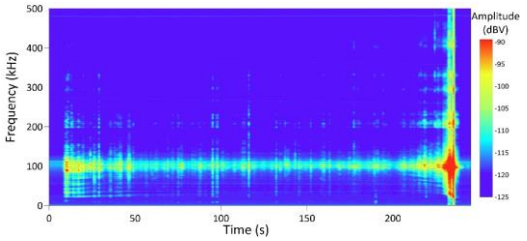

Figure 8. AE behavior under uniaxial compression loading (B-1 specimen)

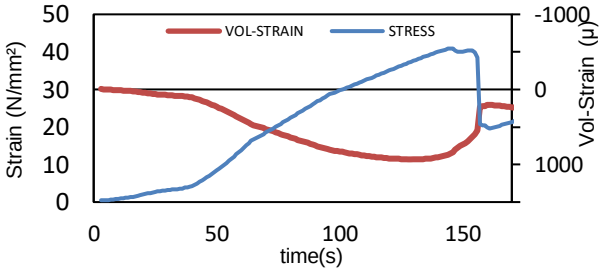

Figure 9. Stress and volumetric strain behavior under uniaxial compression loading (B-2 specimen)

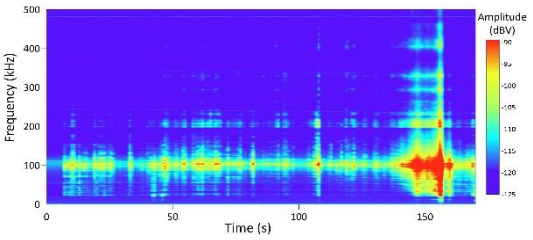

Figure 10. AE behavior under uniaxial compression loading (B-2 specimen)

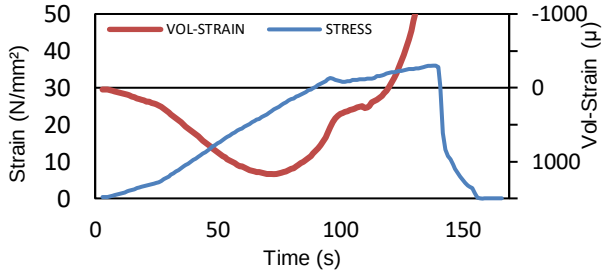

Figure 11. Stress and volumetric strain behavior under uniaxial compression loading (C-1 specimen)

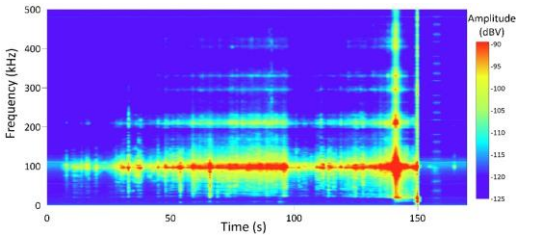

Figure 12. AE behavior under uniaxial compression loading (C-1 specimen)

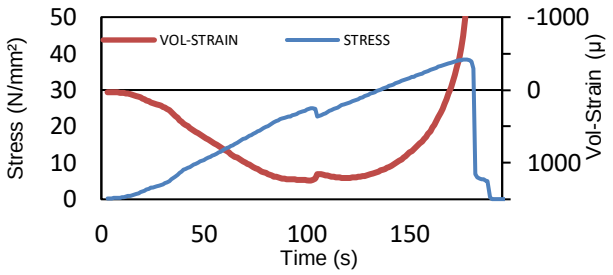

Figure 13. Stress and volumetric strain behavior under uniaxial compression loading (C-2 specimen)

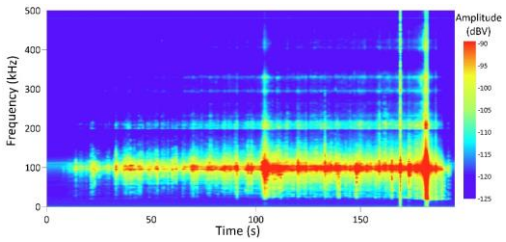

Figure 14. AE behavior under uniaxial compression loading (C-2 specimen)

4 CONCLUTIONS

In this paper, the specimens of polymer cement mortar (PCM) with expansive additive were measured to investigate the expansion and shrinkage behavior during curing. A uniaxial compression test was carried out to investigate the mechanical behavior of the PCM specimen. AE signals were recorded during the uniaxial compression test to investigate the AE behavior under the loading from unloading to failure. Here, the specimens to which no expansive additive was added will be called "sound specimens", and those to which an excessive amount of expansive additive was added will be called "degraded specimens". As a result, the following findings were obtained ;

(1) For the degraded specimens, many AE signals with large amplitude occurred from initial loading to failure. On the other hand, for the sound specimens, there was a little AE signal until the maximum volumetric strain, the number and amplitude of that drastically increased close to failure.

(2) The spectrogram of the degraded specimens had a large amplitude in a relatively wide frequency band from the initial loading. In the spectrogram of the sound specimens, the frequency band with large amplitude gradually increased from the maximum volumetric strain.

(3) The degraded specimens tended to have a larger axial strain of maximum stress and larger maximum volumetric strain than the sound one. In addition, for the degraded specimens, the time between maximum volumetric strain and failure became longer.

5 REFERENCES

Motahari-Nezhad, M. and Mohammad Jafari, S. 2020. ANFIS system for prognosis of dynamometer high-speed ball bearing based on frequency domain acoustic emission signals, *Measurement*, 166: 108154.

Zhang, Y., Teramoto A. and Ohkubo, T. 2018. Effect of addition rate of expansive additive on autogenous shrinkage and delayed expansion of ultra-high strength mortar, *Journal of Advanced Concrete Technology*, Japan Concrete Institute, 16: 250-261.